

The muon anomalous magnetic moment in the supersymmetric economical 3-3-1 model

D. T. Binh*, D. T. Huong[†] and H. N. Long[‡]

*Institute of Physics, Vietnam Academy of Science and Technology,
10 Dao Tan, Ba Dinh, Hanoi, Vietnam*

Abstract

We investigate the muon anomalous magnetic moment in the context of the supersymmetric version of the economical 3-3-1 model. We compute the 1-loop contribution of super-partner particles. We show that the contribution of superparticle loops become significant when $\tan \gamma$ is large. We investigate for both small and large values of $\tan \gamma$. We find the region of the parameter space where the slepton masses are of a few hundreds GeV is favoured by the muon $g - 2$ for small $\tan \gamma$ ($\tan \gamma \sim 5$). Numerical estimation gives the mass of supersymmetric particle, the mass of gauginos $m_G \sim 700$ GeV and light slepton mass $m_{\tilde{L}}$ is of order $\mathcal{O}(100)$ GeV. When $\tan \gamma$ is large ($\tan \gamma \sim 60$), the mass of charged slepton $m_{\tilde{L}}$ and the mass of gauginos $m_G \sim \mathcal{O}(1)$ TeV while the mass of sneutrino ~ 450 GeV is in the reach of LHC.

* dtbinh@iop.vast.ac.vn

[†] dthuong@iop.vast.ac.vn

[‡] hnlong@iop.vast.ac.vn

I. INTRODUCTION

The muon magnetic dipole moment (MDM), written in terms of $a_\mu = \frac{g_\mu - 2}{2}$, is one of the most highly measured quantity in particle physics. The current discrepancy between experimental value and that predicted by Standard Model (SM) $\Delta a_\mu = a_\mu^{(exp)} - a_\mu^{(SM)}$ is 3.6σ [1]. This discrepancy demands an explanation. Efforts in both the experimental and theoretical fronts are taking to address this issue. On the theoretical front, there are models of new physics. One of these models is the class of $SU(3)_C \times SU(3)_L \times U(1)$ (3-3-1) models [2]-[14]. In this class of models, the $SU(2)_L$ gauge symmetry group is extended to $SU(3)_L$ and has some intriguing features: They can give of the generation number problem; dark matter; small neutrinos mass and their mixing and some problems of the Early Universe [15]. Among the 3-3-1 models, there is one version called the economical 3-3-1 model (E331). The economical 3-3-1 model [14] is a model with just two Higgs triplet. The Higgs sector in the E331 model is very simple and consists of two massive neutral Higgs scalars, one massive charged Higgs and eight Goldstone bosons. Because of the expansion of the gauge group, the 3-3-1 models contain new particles such as new Higgs, new gauge bosons as well as new fermions. Due to the interactions of the muon with some new heavy particles, the 3-3-1 models can give new contribution to the muon MDM. The muon MDM problem is also investigated in this class of models [16]- [19]. However this class of models cannot probably explain the $(g - 2)_\mu$ anomaly if the $SU(3)_L$ symmetry breaking scale is larger than $\mathcal{O}(1)$ TeV [20, 33].

Supersymmetry (SUSY) is one of the most promising candidates of the new physics beyond Standard Model. In SUSY models, the Higgs sector is very constrained and the quadratic divergences are cancelled out and hence offer a solution to the naturalness problem [21]. In addition, precision measurements of the gauge coupling constants strongly suggest SUSY grand unified theory [22].

There are works in which the muon MDM is calculated in the framework of SUSY models [23]. In minimal supersymmetric standard model (MSSM) [24], the SUSY contribution is proportional to $\tan \beta$ which is the ratio of the vacuum expectation values of two Higgs fields and suppression factor $\left(\frac{m_\mu}{M_{SUSY}}\right)^2$. If $\tan \beta$ is large then a_μ^{SUSY} can be as large as Δa_μ [1] or if low energy SUSY exists, the SUSY contribution to the muon $g - 2$ can be large enough to address the muon MDM anomaly provided the masses of supersymmetry particle, order

$\mathcal{O}(100 \text{ GeV})$ or $\mathcal{O}(\text{TeV})$, which are in the reach of the LHC. Thus the muon MDM can be possibly originated from SUSY contributions.

It is natural to investigate the muon MDM in the SUSY version of the 3-3-1 models. In this work we will investigate the muon MDM in the framework of the supersymmetric version of the economical 331 model (SUSYE331). The SUSY version of the economical 3-3-1 model (SUSYE331) was proposed in [26]. In the SUSYE331 model the region of parameter space can be expanded comparing to that of the MSSM. The works given in [27, 28] showed that the interested region of parameter space to study the LFV decay process can be expanded to the limit of the small value of $\tan\gamma$ and the slepton mass of at least one generation can be taken in the $\mathcal{O}(100)$ GeV energy scale.

We will first derive the analytical expressions for all one-loop contributions coming from the SUSYE331 and show that the contribution of the SUSYE331 model to the muon MDM is proportional to the values of $\tan\gamma$ and inverse proportional to the values of the slepton masses. We will show the magnitude of contribution to the muon MDM for each choice of the value of the $\tan\gamma$. Because of appearance of new particles in the SUSYE331, we expect finding the interested region of the SUSY parameter space in the limit of the small $\tan\gamma$. We are particularly interested in exploring some numerical results of the SUSYE331 contribution to the muon MDM in the limits where SUSYE331 slepton and gaugino masses are of order TeV and small values of $\tan\gamma$.

The paper is organized as follows. In section 2 we will briefly review the SUSYE331 model. In section III and IV we will go through the neutralinos and charginos sectors of the model. Section V and VI are devoted for diagonalizing the mass matrix of the smuon, sneutrino and the muon-chargino-sneutrino interaction. In section VII we will calculate the muon MDM in the weak eigenstate. Section VIII is devoted for numerical calculation and bounds on masses. We will summarize our results in section IX.

II. A REVIEW OF THE MODEL

In this section we first recapitulate the basic elements of the supersymmetric economical 3-3-1 model [26]. The superfield content in this paper is defined as follows:

$$\widehat{F} = (\tilde{F}, F), \quad \widehat{S} = (S, \tilde{S}), \quad \widehat{V} = (\lambda, V), \quad (1)$$

where the components F , S and V stand for the fermion, scalar and vector fields while their superpartners are denoted as \tilde{F} , \tilde{S} and λ , respectively.

The superfield content of the model with an anomaly-free fermionic content transforms under the 3-3-1 gauge group as

$$\begin{aligned}\hat{L}_{aL} &= \left(\hat{\nu}_a, \hat{l}_a, \hat{\nu}_a^c \right)_L^T \sim (1, 3, -1/3), \quad \hat{l}_{aL}^c \sim (1, 1, 1), \\ \hat{Q}_{1L} &= \left(\hat{u}_1, \hat{d}_1, \hat{u}'_1 \right)_L^T \sim (3, 3, 1/3), \\ \hat{u}_{1L}^c, \hat{u}'_{1L}^c &\sim (3^*, 1, -2/3), \quad \hat{d}_{1L}^c \sim (3^*, 1, 1/3), \\ \hat{Q}_{\alpha L} &= \left(\hat{d}_\alpha, -\hat{u}_\alpha, \hat{d}'_\alpha \right)_L^T \sim (3, 3^*, 0), \quad \alpha = 2, 3, \\ \hat{u}_{\alpha L}^c &\sim (3^*, 1, -2/3), \quad \hat{d}_{\alpha L}^c, \hat{d}'_{\alpha L}^c \sim (3^*, 1, 1/3),\end{aligned}$$

where the values in the parentheses denote quantum numbers based on $(\text{SU}(3)_C, \text{SU}(3)_L, \text{U}(1)_X)$ symmetry. $\hat{\nu}_L^c = (\hat{\nu}_R)^c$ and $a = 1, 2, 3$ is a generation index. The primes superscript on usual quark types (u', d' with the electric charge $q_{u'} = 2/3$ and d' with $q_{d'} = -1/3$) indicate that those quarks are exotic ones.

The two superfields $\hat{\chi}$ and $\hat{\rho}$ are introduced to span the scalar sector of the economical 3-3-1 model [14]:

$$\begin{aligned}\hat{\chi} &= \left(\hat{\chi}_1^0, \hat{\chi}^-, \hat{\chi}_2^0 \right)^T \sim (1, 3, -1/3), \\ \hat{\rho} &= \left(\hat{\rho}_1^+, \hat{\rho}^0, \hat{\rho}_2^+ \right)^T \sim (1, 3, 2/3).\end{aligned}$$

To cancel the chiral anomalies of higgsino sector, two extra superfields $\hat{\chi}'$ and $\hat{\rho}'$ must be added as follows

$$\begin{aligned}\hat{\chi}' &= \left(\hat{\chi}_1'^0, \hat{\chi}'^+, \hat{\chi}_2'^0 \right)^T \sim (1, 3^*, 1/3), \\ \hat{\rho}' &= \left(\hat{\rho}_1'^-, \hat{\rho}'^0, \hat{\rho}_2'^- \right)^T \sim (1, 3^*, -2/3).\end{aligned}$$

In this model, the $\text{SU}(3)_L \otimes \text{U}(1)_X$ gauge group is broken via two steps:

$$\text{SU}(3)_L \otimes \text{U}(1)_X \xrightarrow{w,w'} \text{SU}(2)_L \otimes \text{U}(1)_Y \xrightarrow{v,v',u,u'} \text{U}(1)_Q, \quad (2)$$

where the VEVs are defined by

$$\begin{aligned}\sqrt{2}\langle \chi \rangle^T &= (u, 0, w), \quad \sqrt{2}\langle \chi' \rangle^T = (u', 0, w'), \\ \sqrt{2}\langle \rho \rangle^T &= (0, v, 0), \quad \sqrt{2}\langle \rho' \rangle^T = (0, v', 0).\end{aligned} \quad (3)$$

The VEVs w and w' are responsible for the first step of the symmetry breaking while u , u' and v , v' are for the second one. Therefore, they have to satisfy the constraints:

$$u, u', v, v' \ll w, w'. \quad (4)$$

The vector superfields \hat{V}_c , \hat{V} and \hat{V}' containing the usual gauge bosons are, respectively, associated with the $SU(3)_C$, $SU(3)_L$ and $U(1)_X$ group factors. The colour and flavour vector superfields have expansions in the Gell-Mann matrix bases $T^a = \lambda^a/2$ ($a = 1, 2, \dots, 8$) as follows

$$\hat{V}_c = \frac{1}{2} \lambda^a \hat{V}_{ca}, \bar{\hat{V}}_c = -\frac{1}{2} \lambda^{a*} \hat{V}_{ca}; \hat{V} = \frac{1}{2} \lambda^a \hat{V}_a, \bar{\hat{V}} = -\frac{1}{2} \lambda^{a*} \hat{V}_a,$$

where the overbar $\bar{}$ indicates complex conjugation. The vector superfields associated with $U(1)_X$ are normalized as follows

$$X\hat{V}' = (XT^9)\hat{B}, \quad T^9 \equiv \frac{1}{\sqrt{6}} \text{diag}(1, 1, 1).$$

The gluons are denoted by g^a and their gluino partners by λ_c^a , with $a = 1, \dots, 8$. In the electroweak sector, V^a and B stand for the $SU(3)_L$ and $U(1)_X$ gauge bosons with their gaugino partners λ_V^a and λ_B , respectively.

With the given superfields, the full Lagrangian is defined by $\mathcal{L}_{susy} + \mathcal{L}_{soft}$ where the first term is supersymmetric part, whereas the last term breaks the supersymmetry explicitly. The interested reader can find more details about the Lagrangian in [26]. In the followings, we only interest in terms relevant to our calculations.

III. THE NEUTRALINOS AND CHARGINO SECTORS

In the SUSYE331 the neutralinos are mixed by 11×11 matrix and the charginos are mixed by 5×5 matrix. It is difficult to find the exactly mass eigenstate of these mixing mass matrices. Hence, we have to find the approximation method.

A. The neutralino sector

The neutralino mass terms are given in [30] as follows:

$$\mathcal{L} = (\widetilde{\psi}^o)^\dagger M_{\widetilde{N}} \widetilde{\psi}^o, \quad (5)$$

with

$$\tilde{\psi}^o = \left(\widetilde{\chi}_1^o, \widetilde{\chi}_1^{o'}, \widetilde{\chi}_2^o, \widetilde{\chi}_2^{o'}, \widetilde{\rho}_1^o, \widetilde{\rho}_1^{o'}, \lambda_B, \lambda_3, \lambda_8, \lambda_X = \frac{\lambda_4 + i\lambda_5}{2}, \lambda_{X^*} = \frac{\lambda_4 - i\lambda_5}{2} \right)$$

and the mass matrix $M_{\widetilde{N}}$ has the form as follows

$$M_{\widetilde{N}} = \begin{pmatrix} 0 & -\mu_\chi & 0 & 0 & 0 & 0 & -\frac{g'u}{3\sqrt{6}} & \frac{gu}{2} & \frac{gu}{2\sqrt{3}} & \frac{gw}{\sqrt{2}} & 0 \\ -\mu_\chi & 0 & 0 & 0 & 0 & 0 & \frac{g'u'}{3\sqrt{6}} & \frac{gu'}{2} & \frac{gu'}{2\sqrt{3}} & \frac{gw'}{\sqrt{2}} & 0 \\ 0 & 0 & 0 & & -\mu_\chi & 0 & -\frac{g'w}{3\sqrt{6}} & 0 & -\frac{gw}{\sqrt{3}} & 0 & \frac{gu}{\sqrt{2}} \\ 0 & 0 & -\mu_\chi & 0 & 0 & 0 & \frac{g'w'}{3\sqrt{6}} & 0 & -\frac{gw'}{\sqrt{3}} & 0 & \frac{gu'}{\sqrt{2}} \\ 0 & 0 & 0 & 0 & 0 & -\mu_\rho & \frac{2g'v}{3\sqrt{6}} & -\frac{gv}{2} & \frac{gv}{2\sqrt{3}} & 0 & 0 \\ 0 & 0 & 0 & 0 & -\mu_\rho & 0 & -\frac{2g'v'}{3\sqrt{6}} & -\frac{gv'}{2} & \frac{gv'}{2\sqrt{3}} & 0 & 0 \\ -\frac{g'u}{3\sqrt{6}} & \frac{g'u'}{3\sqrt{6}} & -\frac{g'w}{3\sqrt{6}} & \frac{g'w'}{3\sqrt{6}} & \frac{2g'v}{3\sqrt{6}} & -\frac{2g'v'}{3\sqrt{6}} & m_B & 0 & 0 & 0 & 0 \\ \frac{gu}{2} & \frac{gu'}{2} & 0 & 0 & -\frac{gv}{2} & -\frac{gv'}{2} & 0 & m_{\lambda_3} & 0 & 0 & 0 \\ \frac{gu}{2\sqrt{3}} & \frac{gu'}{2\sqrt{3}} & -\frac{gw}{\sqrt{3}} & -\frac{gw'}{\sqrt{3}} & \frac{gv}{2\sqrt{3}} & \frac{gv'}{2\sqrt{3}} & 0 & 0 & m_{\lambda_8} & 0 & 0 \\ \frac{gw}{2} & \frac{gw'}{2} & 0 & 0 & 0 & 0 & 0 & 0 & 0 & m_{\lambda_{45}} & 0 \\ 0 & 0 & \frac{gu}{2} & \frac{gu'}{2} & 0 & 0 & 0 & 0 & 0 & 0 & m_{\lambda_{45}} \end{pmatrix}, \quad (6)$$

where $m_{\lambda_4} = m_{\lambda_5} \equiv m_{\lambda_{45}}$.

In general, we can find a new basis in which the mass matrix $M_{\widetilde{N}}$ has the diagonal form by finding an unitary matrix N satisfied

$$N^* M_{\widetilde{N}} N^\dagger = \text{Diag}(m_{\widetilde{\chi}_1}^2, m_{\widetilde{\chi}_2}^2, m_{\widetilde{\chi}_3}^2, m_{\widetilde{\chi}_4}^2, m_{\widetilde{\chi}_5}^2, m_{\widetilde{\chi}_6}^2, m_{\widetilde{\chi}_7}^2, m_{\widetilde{\chi}_8}^2, m_{\widetilde{\chi}_9}^2, m_{\widetilde{\chi}_{10}}^2, m_{\widetilde{\chi}_{11}}^2).$$

As have done in [30], we assume that

$$v, v', u, u', w, w' \ll |\mu_\rho - m_B|, |\mu_\rho - m_{\lambda_3}|, |\mu_\rho - m_{\lambda_8}|, |\mu_\rho - m_{\lambda_{45}}| \quad (7)$$

and

$$v, v', u, u', w, w' \ll |\mu_\chi - m_B|, |\mu_\chi - m_{\lambda_3}|, |\mu_\chi - m_{\lambda_8}|, |\mu_\chi - m_{\lambda_{45}}|. \quad (8)$$

In these limits, we get the neutralino mass eigenstates by using perturbation. At the first

order of the perturbation, we obtain the mixing matrix N such as:

$$N = \begin{pmatrix} 0 & 0 & 0 & 0 & 0 & 0 & 1 & 0 & 0 & 0 & 0 \\ 0 & 0 & 0 & 0 & 0 & 0 & 0 & 1 & 0 & 0 & 0 \\ 0 & 0 & 0 & 0 & 0 & 0 & 0 & 0 & 1 & 0 & 0 \\ 0 & 0 & 0 & 0 & 0 & 0 & 0 & 0 & 0 & 1 & 0 \\ 0 & 0 & 0 & 0 & 0 & 0 & 0 & 0 & 0 & 0 & 1 \\ 0 & 0 & 0 & 0 & 0 & 0 & 0 & 0 & 0 & 0 & 0 \\ 0 & 0 & 0 & 0 & 0 & \frac{1}{\sqrt{2}} & \frac{1}{\sqrt{2}} & 0 & 0 & 0 & 0 \\ 0 & 0 & 0 & 0 & 0 & \frac{1}{\sqrt{2}} & -\frac{1}{\sqrt{2}} & 0 & 0 & 0 & 0 \\ \frac{1}{\sqrt{2}} & \frac{1}{\sqrt{2}} & 0 & 0 & 0 & 0 & 0 & 0 & 0 & 0 & 0 \\ \frac{1}{\sqrt{2}} & -\frac{1}{\sqrt{2}} & 0 & 0 & 0 & 0 & 0 & 0 & 0 & 0 & 0 \\ 0 & 0 & \frac{1}{\sqrt{2}} & \frac{1}{\sqrt{2}} & 0 & 0 & 0 & 0 & 0 & 0 & 0 \\ 0 & 0 & \frac{1}{\sqrt{2}} & -\frac{1}{\sqrt{2}} & 0 & 0 & 0 & 0 & 0 & 0 & 0 \end{pmatrix},$$

and the mass eigenvalues as studied in [30].

B. Chargino sector

In the SUSYE331 model, there are four charged gauginos and six charged Higgsinos. In the basis $\psi^+ = (\lambda_{\tilde{W}^+}, \lambda_{\tilde{Y}^+}, \tilde{\rho}_1^+, \tilde{\rho}_2^+, \tilde{\chi}'^+)$, $\psi^- = (\lambda_{\tilde{W}^-}, \lambda_{\tilde{Y}^-}, \tilde{\rho}_1'^-, \tilde{\rho}_2'^-, \tilde{\chi}^-)$, the Lagrangian describes the chargino mass terms is given as follows

$$\mathcal{L}_{charginomass} = (\tilde{\psi}^\pm)^+ M_{\tilde{\psi}} \tilde{\psi}^\pm + H.c,$$

with the $M_{\tilde{\psi}}$

$$M_{\tilde{\psi}} = \begin{pmatrix} 0 & \mathcal{M} \\ \mathcal{M}^T & 0 \end{pmatrix},$$

where \mathcal{M} is 5×5 matrix given by

$$\mathcal{M} = \begin{pmatrix} m_{\lambda_W} & 0 & \frac{gv'}{\sqrt{2}} & 0 & \frac{gu}{\sqrt{2}} \\ 0 & m_{\lambda_Y} & 0 & \frac{gv'}{\sqrt{2}} & \frac{gw}{\sqrt{2}} \\ \frac{gv}{\sqrt{2}} & 0 & \mu_\rho & 0 & 0 \\ 0 & \frac{gv}{\sqrt{2}} & 0 & \mu_\rho & 0 \\ \frac{gu'}{\sqrt{2}} & \frac{gw'}{\sqrt{2}} & 0 & 0 & \mu_\chi \end{pmatrix}.$$

In order to diagonalize charginos mass matrix, we have to find two unitary 5×5 matrices U and V such that they satisfy

$$U^* \mathcal{M} V^\dagger = \begin{pmatrix} m_{\lambda_W} & 0 & 0 & 0 & 0 \\ 0 & m_2 & 0 & 0 & 0 \\ 0 & 0 & \mu_\rho & 0 & 0 \\ 0 & 0 & 0 & m_3 & 0 \\ 0 & 0 & 0 & 0 & \mu_\rho \end{pmatrix} \equiv \text{Diag}(m_{\chi_1}^\pm, m_{\chi_2}^\pm, m_{\chi_3}^\pm, m_{\chi_4}^\pm, m_{\chi_5}^\pm),$$

where

$$\begin{aligned} m_2 &= \frac{1}{4} \left[2(\mu_\chi^2 + m_{\lambda_Y}^2) + g^2(w^2 + w'^2) \right. \\ &\quad \left. - \sqrt{(2(\mu_\chi + m_{\lambda_Y})^2 + g^2(w - w')^2)(2(\mu_\chi - m_{\lambda_Y})^2 + g^2(w + w')^2)} \right], \\ m_3 &= \frac{1}{4} \left[2(\mu_\chi^2 + m_{\lambda_Y}^2) + g^2(w^2 + w'^2) \right. \\ &\quad \left. + \sqrt{(2(\mu_\chi + m_{\lambda_Y})^2 + g^2(w - w')^2)(2(\mu_\chi - m_{\lambda_Y})^2 + g^2(w + w')^2)} \right]. \end{aligned}$$

In order to find the matrices U, V we have to diagonalize the matrix $M^\dagger M$ by finding the matrix C such that it satisfies $C^\dagger M^\dagger M C \equiv M_D^2$, M_D has a diagonal form. Meanwhile, the shape of the matrices U and V are represented through the matrices U, V as follows

$$V^\dagger = C, \quad U^* = M_D^{-1} C^\dagger M^\dagger.$$

In the leading order $m_{\lambda_W}, m_{\lambda_Y}, \mu_\rho, \mu_\chi, w, w' \gg u, u'v, v'$, the matrix C has a form such as

$$C = \begin{pmatrix} 1 & 0 & 0 & 0 & 0 \\ 0 & \frac{A}{\sqrt{1+A^2}} & 0 & \frac{B}{\sqrt{1+B^2}} & 0 \\ 0 & 0 & 1 & 0 & 0 \\ 0 & 0 & 0 & 0 & 1 \\ 0 & \frac{1}{\sqrt{1+A^2}} & 0 & \frac{1}{\sqrt{1+B^2}} & 0 \end{pmatrix},$$

and the form of the matrix U^* is

$$U^* = \begin{pmatrix} 1 & 0 & \frac{gv}{\sqrt{2m_{\lambda_W}}} & 0 & \frac{gu'}{\sqrt{2m_{\lambda_W}}} \\ \frac{gu}{\sqrt{2(1+A^2)^2m_2}} & \frac{2Am_{\lambda_Y}+\sqrt{2}gw}{2\sqrt{(1+A^2)m_2}} & 0 & \frac{gvA}{\sqrt{2(1+A^2)m_2}} & \frac{2\mu_\chi+\sqrt{2}Agw'}{2\sqrt{(1+A^2)m_2}} \\ \frac{gv'}{\sqrt{2}\mu_\rho} & 0 & 1 & 0 & 0 \\ \frac{gu}{\sqrt{2(1+B^2)m_3}} & \frac{2Bm_{\lambda_Y}+\sqrt{2}gw}{2\sqrt{(1+B^2)m_3}} & 0 & \frac{Bgv}{\sqrt{2(1+B^2)m_3}} & \frac{2\mu_\chi+\sqrt{2}gw'B}{\sqrt{2(1+B^2)m_3}} \\ 0 & \frac{gv'}{\sqrt{2}\mu_\rho} & 0 & 1 & 0 \end{pmatrix}$$

where

$$\begin{aligned}
A &= \frac{1}{2\sqrt{2}(m_{\lambda_Y}w + \mu_\chi w')} \left(2(\mu_\chi^2 - m_{\lambda_Y}^2) + g^2(w^2 - w'^2) \right. \\
&\quad \left. + \sqrt{-4(-2\mu_\chi m_{\lambda_Y} + g^2 w w')^2 + (2(\mu_\chi^2 + m_{\lambda_Y}^2) + g^2(w^2 + w'^2))^2} \right), \\
B &= \frac{1}{2\sqrt{2}(m_{\lambda_Y}w + \mu_\chi w')} \left(-2(\mu_\chi^2 - m_{\lambda_Y}^2) - g^2(w^2 - w'^2) \right. \\
&\quad \left. + \sqrt{-4(-2\mu_\chi m_{\lambda_Y} + g^2 w w')^2 + (2(\mu_\chi^2 + m_{\lambda_Y}^2) + g^2(w^2 + w'^2))^2} \right).
\end{aligned}$$

IV. SMUON AND SNEUTRINO MASSES

The superpotential of the model under consideration relevant to the contribution of $(g-2)_\mu$ is given as follows:

$$W' = \mu_{0a} \hat{L}_{aL} \hat{\chi}' + \mu_\chi \hat{\chi} \hat{\chi}' + \mu_\rho \hat{\rho} \hat{\rho}' + \gamma_{ab} \hat{L}_{aL} \hat{\rho}' \hat{l}_{bL}^c + \lambda_a \epsilon \hat{L}_{aL} \hat{\chi} \hat{\rho} + \lambda'_{ab} \epsilon \hat{L}_{aL} \hat{L}_{bL} \hat{\rho},$$

with μ_{0a} , μ_ρ and μ_χ have mass dimension, the other coefficients in W' are dimensionless and $\lambda'_{ab} = -\lambda'_{ba}$.

Relevant soft breaking terms are obtained by

$$\begin{aligned}
-\mathcal{L}_{SMT} &= M_{ab}^2 \tilde{L}_{aL}^\dagger \tilde{L}_{bL} + m_{ab}^2 \tilde{l}_{aL}^{c*} \tilde{l}_{bL}^c + \left\{ M_a'^2 \chi^\dagger \tilde{L}_{aL} + \eta_{ab} \tilde{L}_{aL} \rho' \tilde{l}_{bL}^c + v_a \epsilon \tilde{L}_{aL} \chi \rho \right. \\
&\quad \left. + \varepsilon_{ab} \epsilon \tilde{L}_{aL} \tilde{L}_{bL} \rho + \omega_{a\alpha j} \tilde{L}_{aL} \tilde{Q}_{\alpha L} \tilde{d}_{jL}^c + \omega'_{a\alpha\beta} \tilde{L}_{aL} \tilde{Q}_{\alpha L} \tilde{d}_{\beta L}^c + H.c. \right\},
\end{aligned} \tag{9}$$

where $\varepsilon_{ab} = -\varepsilon_{ba}$. This Lagrangian is also responsible for sfermion masses. The sfermion masses are obtained by combining of the soft terms, D-terms and F-terms. The interested reader can see in [29]. In general, there are flavour mixing in slepton mass matrix. However, the large flavour mixing in slepton sector can create a mismatch for the lepton flavor decay processes of muon and tauon [27, 28]. In this work, we assume that the flavour mixing matrix elements are not so large. We can ignore all the flavour mixing terms. The mass matrix for smuon can be written as

$$M_{smuon} = \begin{pmatrix} m_{\tilde{\mu}L}^2 & m_{\tilde{\mu}LR}^2 \\ m_{\tilde{\mu}LR}^2 & m_{\tilde{\mu}R}^2 \end{pmatrix}, \tag{10}$$

where

$$m_{\tilde{\mu}L}^2 = M_{22}^2 + \frac{1}{4}\mu_{02}^2 + \frac{g^2}{2} \left(-H_3 + \frac{1}{\sqrt{3}}H_8 - \frac{2t^2}{3}H_1 \right) + \frac{v'^2}{18}\gamma_{22}^2 + \frac{1}{18}\lambda_2^2(u^2 + w^2), \tag{11}$$

$$\begin{aligned} m_{\mu R}^2 &= \left(m_{22}^2 + \frac{v'^2}{18} \gamma_{22}^2 + g^2 t^2 H_1 \right), \\ m_{\tilde{\mu} LR}^2 &= \frac{1}{\sqrt{2}} \left(\eta_{22} v' + \frac{1}{6} \mu_\rho \gamma_2 v \right), \end{aligned} \quad (12)$$

with

$$H_3 = -\frac{1}{4} \left(u^2 \frac{\cos 2\beta}{s_\beta^2} + v^2 \frac{\cos 2\gamma}{c_\gamma^2} \right), \quad (13)$$

$$H_8 = \frac{1}{4\sqrt{3}} \left[v^2 \frac{\cos 2\gamma}{c_\gamma^2} - (u^2 - 2w^2) \frac{\cos 2\beta}{s_\beta^2} \right], \quad (14)$$

$$H_4 = -\frac{1}{2} uw \frac{\cos 2\beta}{s_\beta^2}, \quad (15)$$

$$H_1 = \frac{1}{6} \left[(u^2 + w^2) \frac{\cos 2\beta}{s_\beta^2} + 2v^2 \frac{\cos 2\gamma}{c_\gamma^2} \right], \quad (16)$$

$$\text{and } \tan \beta = \frac{u}{u'} = \frac{w}{w'}, \quad \tan \gamma = \frac{v'}{v}, \quad s_\beta = \sin \beta, \quad c_\beta = \cos \beta.$$

Diagonalizing the mass matrix given in Eq.(10), we can obtain the mass eigenvalues as follows:

$$m_{\tilde{\mu} L}^2 = \frac{1}{2} (m_{\tilde{\mu} L}^2 + m_{\tilde{\mu} R}^2 - \Delta), \quad (17)$$

$$m_{\tilde{\mu} R}^2 = \frac{1}{2} (m_{\tilde{\mu} L}^2 + m_{\tilde{\mu} R}^2 + \Delta), \quad (18)$$

$$\text{where } \Delta = \sqrt{(m_{\tilde{\mu} L}^2 - m_{\tilde{\mu} R}^2)^2 + 4m_{\tilde{\mu} LR}^4}.$$

The mass eigenstates are given, respectively

$$\begin{aligned} \begin{pmatrix} \tilde{\mu}_L \\ \tilde{\mu}_R \end{pmatrix} &= \begin{pmatrix} s_{\theta_\mu} & -c_{\theta_\mu} \\ c_{\theta_\mu} & s_{\theta_\mu} \end{pmatrix} \begin{pmatrix} l_{\tilde{\mu} R} \\ l_{\tilde{\mu} L} \end{pmatrix} \equiv U_{\tilde{\mu}}^{-1} \begin{pmatrix} l_{\tilde{\mu} R} \\ l_{\tilde{\mu} L} \end{pmatrix} \\ \tilde{\mu}_L &= c_{\theta_\mu} l_{\tilde{\mu} R} - s_{\theta_\mu} l_{\tilde{\mu} L}, \\ \tilde{\mu}_R &= s_{\theta_\mu} l_{\tilde{\mu} R} + c_{\theta_\mu} l_{\tilde{\mu} L}, \end{aligned} \quad (19)$$

$$\begin{aligned} \text{with } s_{\theta_\mu} &= \sin \theta_\mu, \quad c_{\theta_\mu} = \cos \theta_\mu \text{ and the } \theta_\mu \text{ is defined through } \tan 2\theta_\mu = \\ t_{2\theta_\mu} &= \frac{2m_{\tilde{\mu} L}^2}{m_{\tilde{\mu} L}^2 - m_{\tilde{\mu} R}^2}. \end{aligned}$$

Next, We will study the muon sneutrino mass. If we ignore mixing among sneutrinos of two first generations, the mass of the sneutrino $m_{\tilde{\nu}_\mu}$ has the form

$$m_{\tilde{\nu}_{\mu L}}^2 = M_{22}^2 + \frac{1}{4} \mu_{02}^2 + \frac{g^2}{2} \left(H_3 + \frac{1}{\sqrt{3}} H_8 - \frac{2t^2}{3} H_1 \right) + \frac{1}{18} v^2 (\lambda_2^2 + 4\lambda_{c2}^{\prime 2}) + \frac{1}{18} \lambda_2^2 w^2, \quad (20)$$

$$m_{\tilde{\nu}_{\mu R}}^2 = M_{22}^2 + \frac{1}{4} \mu_{02}^2 - g^2 \left(\frac{1}{\sqrt{3}} H_8 + \frac{t^2}{3} H_1 \right) + \frac{1}{18} v^2 (\lambda_2^2 + 4\lambda_{c2}^{\prime 2}) + \frac{1}{18} \lambda_2^2 u^2. \quad (21)$$

V. MUON NEUTRALINO SMUON AND MUON CHARGINO SNEUTRINO VERTICES.

The interaction terms contain the lepton neutralino slepton and lepton chargino sneutrino vertices are given as follows:

$$L_{\tilde{u}\tilde{V}} = -\frac{ig}{\sqrt{2}} \left(\bar{L} \lambda^a \tilde{L} \bar{\lambda}_V^a - \bar{\tilde{L}} \lambda^a L \lambda_V^a \right) - ig' \sqrt{\frac{1}{3}} \left[-\frac{1}{3} (\bar{L} \tilde{L} \bar{\lambda}_B - \bar{\tilde{L}} L \lambda_B) + (\bar{l}^c \tilde{l}^c \bar{\lambda}_B - \bar{\tilde{l}} l^c \lambda_B) \right], \quad (22)$$

$$L_{\tilde{u}\tilde{H}} = -\frac{\lambda_{1ab}}{3} \left(L_a \tilde{\rho}' \tilde{l}_b^c + \tilde{L}_a \tilde{\rho}' l_b^c \right) - \frac{\lambda_{3ab}}{3} \left(L_a \tilde{\rho} \tilde{L}_b + \tilde{L}_a \tilde{\rho} L_b \right) + H.c. \quad (23)$$

We would like to remind that the lepton number is conserved in the lepton sector at the tree level and λ_{3ab} are antisymmetric with a and b leading to the vanish of couplings $\lambda_{1ab}, \lambda_{3ab}$ if a equals to b . We use the notations $Y_\mu = \frac{\lambda_{122}}{3}$ as given in [28]. Expanding the Eqs. (22) and (23), we rewrite only the muon-neutralino-smuon and muon-chargino-sneutrino interaction terms. All relevant terms are given as

$$\begin{aligned} L_{\mu\tilde{\mu}\tilde{V}} &= \bar{\mu}_L \left(\frac{ig'}{3\sqrt{3}} \bar{\lambda}_B + \frac{ig}{\sqrt{2}} (\bar{\lambda}_A^3 - \frac{1}{\sqrt{3}} \bar{\lambda}_A^8) \right) \tilde{\mu}_L - \mu_L \left(\frac{ig'}{3\sqrt{3}} \lambda_B + \frac{ig}{\sqrt{2}} (\lambda_A^3 - \frac{1}{\sqrt{3}} \lambda_A^8) \right) \tilde{\mu}_L^* \\ &\quad - i \frac{g'}{\sqrt{3}} (\bar{\mu}^c \tilde{\mu}^c \bar{\lambda}_B - \bar{\tilde{\mu}}^c \mu^c \lambda_B) - ig \left(\bar{\mu}_L \bar{\tilde{W}}^+ \tilde{\nu}_{\mu L} - \mu_L \tilde{W}^+ \tilde{\nu}_{\mu L}^* \right) \\ &\quad + ig \left(\bar{\mu}_L \bar{\tilde{Y}}^+ \tilde{\nu}_{\mu L} - \mu_L \tilde{Y}^+ \tilde{\nu}_{\mu L}^* \right). \end{aligned} \quad (24)$$

$$L_{\mu\tilde{\mu}\tilde{H}} = -Y_\mu \{ \mu_L \tilde{\mu}_L^c \tilde{\rho}'^o + \tilde{\mu}_L \tilde{\rho}'^o \mu_L^c + \tilde{\nu}_{\mu L} \tilde{\rho}_1'^- \mu_L^c + \tilde{\nu}_{\mu L}^c \tilde{\rho}_2'^- \mu_L^c \} + H.c. \quad (25)$$

The Eqs. (24), (25) can be written in the physical states as follows:

$$L_{\mu\tilde{\mu}\chi_i} = \sum_{iA} \bar{\mu} (P_R N_{\chi_i \tilde{\mu}_A}^R + P_L N_{\chi_i \tilde{\mu}_A}^L) \tilde{\mu}_A \bar{\chi}_i + \sum_{jB} \bar{\mu} (P_R C_{\chi_j \tilde{\nu}_B}^R + P_L C_{\chi_j \tilde{\nu}_B}^L) \bar{\chi}_j^+ \tilde{\nu}_A + H.c, \quad (26)$$

where

$$\begin{aligned} N_{\chi_i \tilde{\mu}_A}^L &= \left(\frac{ig'}{3\sqrt{3}} N_{7i}^* + \frac{ig}{\sqrt{2}} N_{8i}^* - \frac{ig}{\sqrt{6}} N_{9i}^* \right) \times (U_{\tilde{\mu}})_{LA} - Y_\mu N_{6i}^* (U_{\tilde{\mu}})_{RA}, \\ N_{\chi_i \tilde{\mu}_A}^R &= -\frac{ig'}{\sqrt{3}} N_{7i}^* (U_{\tilde{\mu}})_{RA} - Y_\mu N_{6i}^* (U_{\tilde{\mu}})_{LA}, \\ C_{\chi_j \tilde{\nu}_B}^L &= -ig (V_{1j} (U_\nu)_{LB} + V_{2j} (U_\nu)_{RB}), \\ C_{\chi_j \tilde{\nu}_B}^R &= -Y_\mu (U_{3j} (U_\nu)_{LA} + U_{4j} (U_\nu)_{RA}). \end{aligned}$$

VI. THE SUSY CONTRIBUTION TO THE MUON MDM

The amplitude for the photon-muon-muon coupling in the zero limit of the momentum of photon can be written as:

$$M_{fi} = ie\bar{u} \left[\gamma^\alpha + a_\mu \frac{i\sigma^{\alpha\beta}q_\beta}{2m_\mu} \right] u A_\alpha$$

The magnetic dipole moment a_μ can be calculated in both mass eigenstate and weak eigenstate. However in the next section the magnetic dipole moment will be evaluated in the weak eigenstate, since in this basis the dependence of a_μ on SUSY parameters is more reveal than in mass eigenstate basis.

The SM prediction of the muon anomalous magnetic moment has been given in [31]

$$a_\mu^{SM} = 116591803(1)(42)(26) \times 10^{-11}$$

The recent E821 experiments [32] have measured and take into account correlations between systematic errors one finds

$$\begin{aligned} a_\mu^{E821} &= 116592091(54)(33) \times 10^{-11} \\ &= (116592091 \pm 63.3) \times 10^{-11} \end{aligned}$$

Hence

$$\begin{aligned} \Delta a_\mu(E821 - SM) &= 288(63)(49) \times 10^{-11} \\ &= (288 \pm 80) \times 10^{-11} \end{aligned}$$

Then we have Δa_μ are 3.68×10^{-9} and 2.08×10^{-9} with the differences 3.6σ and 2.0σ , respectively.

A. Mass eigenstate

The effect of supersymmetry on a_μ includes loops with charginos and neutralinos. The one-loop contributions to a_μ [23], including the effects of possible complex phase, are:

$$\Delta a_\mu^{\chi^0\tilde{\mu}} = m_\mu \sum_{iA} \left\{ -m_\mu (|N_{\chi i\tilde{\mu}A}^L|^2 + |N_{\chi i\tilde{\mu}A}^R|^2) m_{\tilde{\mu}A}^2 \times J_5(m_{\chi i}^2, m_{\tilde{\mu}A}^2, m_{\tilde{\mu}A}^2, m_{\tilde{\mu}A}^2, m_{\tilde{\mu}A}^2) \right\}$$

$$\begin{aligned}
& + m_{\chi_i} \text{Re}(N_{\chi_i \tilde{\mu}_A}^{L*} N_{\chi_i \tilde{\mu}_A}^R) J_4(m_{\chi_i}^2, m_{\chi_i}^2, m_{\tilde{\mu} A}^2, m_{\tilde{\mu} A}^2) \\
& = \frac{1}{16\pi^2} m_\mu \sum_{iA} \left\{ -\frac{m_\mu}{6m_{\tilde{\mu} A}^2(1-x_{\chi_i A})^4} (|N_{\chi_i \tilde{\mu}_A}^L|^2 + |N_{\chi_i \tilde{\mu}_A}^R|^2) \times (1 - 6x_{\chi_i A} + 3x_{\chi_i A}^2 \right. \\
& + 2x_{\chi_i A}^3 - 6x_{\chi_i A}^2 \ln x_{\chi_i A}) - \frac{m_{\chi_i}}{m_{\tilde{\mu} A}^2(1-x_{\chi_i A})^3} \text{Re}(N_{\chi_i \tilde{\mu}_A}^{L*} N_{\chi_i \tilde{\mu}_A}^R) \\
& \times (1 - x_{\chi_i A}^2 + 2x_{\chi_i A} \ln x_{\chi_i A}) \Big\}, \\
\Delta a_\mu^{\chi^\pm \bar{\nu}} & = m_\mu \sum_i \left[m_\mu (|C_{\chi_i \bar{\nu}}^L|^2 + |C_{\chi_i \bar{\nu}}^R|^2) \times \{m_{\bar{\nu}}^2 J_5(m_{\chi_i^\pm}^2, m_{\chi_i^\pm}^2, m_{\chi_i^\pm}^2, m_{\chi_i^\pm}^2, m_{\bar{\nu}}^2) \right. \\
& + J_4(m_{\chi_i^\pm}^2, m_{\chi_i^\pm}^2, m_{\chi_i^\pm}^2, m_{\chi_i^\pm}^2), -J_4(m_{\chi^\pm X}^2, m_{\chi^\pm X}^2, m_{\chi^\pm X}^2 m_{\bar{\nu}}^2) \} \\
& - 2m_X \text{Re}(C_{\chi_i \bar{\nu}}^{L*} C_{\chi_i \bar{\nu}}^R) J_4(m_{\chi_i^\pm X}^2, m_{\chi_i^\pm X}^2, m_{\chi_i^\pm X}^2, m_{\bar{\nu}}^2) \Big] \\
& = \frac{1}{16\pi^2} m_\mu \sum_i \left\{ \frac{m_\mu}{3m_{\bar{\nu}}^2(1-x_{\chi_i^\pm})^4} (|C_{\chi_i \bar{\nu}}^L|^2 + |C_{\chi_i \bar{\nu}}^R|^2) \right. \\
& \times \left(1 + \frac{3}{2}x_{\chi_i^\pm} - 3x_{\chi_i^\pm}^2 + \frac{1}{2}x_{\chi_i^\pm}^3 + 3x_{\chi_i^\pm} \ln x_{\chi_i^\pm} \right) \\
& \left. - \frac{3m_{\chi_i^\pm}}{m_{\bar{\nu}}^2(1-x_{\chi_i^\pm})^3} \text{Re}(C_{\chi_i \bar{\nu}}^{L*} C_{\chi_i \bar{\nu}}^R) \left(1 - \frac{4}{3}x_{\chi_i^\pm} + \frac{1}{3}x_{\chi_i^\pm}^2 + \frac{2}{3} \ln x_{\chi_i^\pm} \right) \right\}, \quad (27)
\end{aligned}$$

where $x_{\chi_i^\pm} = m_{\chi_i^\pm}^2/m_{\bar{\nu}}^2$, $x_{\chi_i A} = m_{\chi_i}^2/m_{\tilde{\mu} A}^2$.

Based on the contributions of SUSYE331 to the muon MDM given in the Eqs. (27), (27), it is hard to see the effects of the SUSYE331 parameter space to the muon MDM, in particular, the role of $\tan \gamma$. To assess the effects of SUSYE331 parameter space to the muon MDM, it is convenient to use the mass insertion method to calculate the diagrams. In next part, let us consider the muon MDM based on the weak eigenstate.

B. Weak eigenstate

In this section, let us consider the SUSY contribution to the muon MDM by using the mass insertion method to calculate the diagrams in Fig. 12,13,14. The contributions to a_μ can be separated into six parts: $a_\mu^{\text{SUSYE331}} = a_{\mu L}^{(a)} + a_{\mu R}^{(a)} + a_{\mu L}^{(b)} + a_{\mu R}^{(b)} + a_{\mu L}^{(c)} + a_{\mu R}^{(c)}$, where diagrams involving each part are expressed in three Figs.12, 13 and 14. Their contributions are given as follows:

$$\begin{aligned}
a_{\mu L}^{(a)} & = -\frac{g^2 m_\mu^2}{8\pi^2} \left[\frac{m_{\tilde{l}_{L2}}^2 c_L^2}{3} J_5(m_\lambda^2, m_{\tilde{l}_{L2}}^2, m_{\tilde{l}_{L2}}^2, m_{\tilde{l}_{L2}}^2, m_{\tilde{l}_{L2}}^2) \right. \\
& \left. - \frac{m_\lambda^2 c_{\nu_L}^2}{2} J_5(m_\lambda^2, m_\lambda^2, m_\lambda^2, m_\lambda^2, m_{\tilde{\nu}_{L2}}^2) \right]
\end{aligned}$$

$$\begin{aligned}
& + \frac{g^2 c_{\nu_R}^2 m_\mu^2}{8\pi^2} \frac{m_\lambda^2}{2} J_5(m_\lambda^2, m_\lambda^2, m_\lambda^2, m_\lambda^2, m_{\tilde{\nu}_{R2}}^2) \\
& - \frac{g'^2 c_L^2 m_\mu^2}{8\pi^2} \frac{m_{\tilde{l}_{L2}}^2}{54} J_5(m_B^2, m_{\tilde{l}_{L2}}^2, m_{\tilde{l}_{L2}}^2, m_{\tilde{l}_{L2}}^2, m_{\tilde{l}_{L2}}^2) \\
& + \left(L_2 \rightarrow L_3, R_2 \rightarrow R_3, c_L^2 \rightarrow s_L^2, c_{\nu_R}^2 \rightarrow s_{\nu_R}^2 \right), \tag{28}
\end{aligned}$$

$$a_{\mu R}^{(a)} = -\frac{g'^2 c_R^2 m_\mu^2}{8\pi^2} \frac{m_{\tilde{l}_{R2}}^2}{6} J_5(m_B^2, m_{\tilde{l}_{R2}}^2, m_{\tilde{l}_{R2}}^2, m_{\tilde{l}_{R2}}^2, m_{\tilde{l}_{R2}}^2) + \left(R_2 \rightarrow R_3, c_R^2 \rightarrow s_R^2 \right), \tag{29}$$

$$\begin{aligned}
a_{\mu L}^{(b)} &= \frac{g^2 c_{\nu_L}^2 m_\mu^2}{8\pi^2} m_{\tilde{\nu}_{L2}}^4 I_5(m_\lambda^2, \mu_\rho^2, m_{\tilde{\nu}_{L2}}^2, m_{\tilde{\nu}_{L2}}^2, m_{\tilde{\nu}_{L2}}^2) \\
&+ \frac{g^2 c_{\nu_R}^2 m_\mu^2}{8\pi^2} m_{\tilde{\nu}_{R2}}^4 I_5(m_\lambda^2, \mu_\rho^2, m_{\tilde{\nu}_{R2}}^2, m_{\tilde{\nu}_{R2}}^2, m_{\tilde{\nu}_{R2}}^2) \\
&- \frac{g^2 c_{\nu_L}^2 m_\mu^2}{8\pi^2} m_\lambda \mu_\rho \tan \gamma \left[J_5(m_\lambda^2, m_\lambda^2, \mu_\rho^2, \mu_\rho^2, m_{\tilde{\nu}_{L2}}^2) + J_5(m_\lambda^2, m_\lambda^2, m_\lambda^2, \mu_\rho^2, m_{\tilde{\nu}_{L2}}^2) \right. \\
&\left. + J_5(m_\lambda^2, \mu_\rho^2, \mu_\rho^2, \mu_\rho^2, m_{\tilde{\nu}_{L2}}^2) \right] - \frac{g^2 c_{\nu_R}^2 m_\mu^2}{8\pi^2} m_\lambda \mu_\rho \tan \gamma \left[J_5(m_\lambda^2, m_\lambda^2, \mu_\rho^2, \mu_\rho^2, m_{\tilde{\nu}_{R2}}^2) \right. \\
&\left. + J_5(m_\lambda^2, m_\lambda^2, m_\lambda^2, \mu_\rho^2, m_{\tilde{\nu}_{R2}}^2) + J_5(m_\lambda^2, \mu_\rho^2, \mu_\rho^2, \mu_\rho^2, m_{\tilde{\nu}_{R2}}^2) \right] \\
&+ \frac{g^2 c_L^2 m_\mu^2}{8\pi^2} m_{\tilde{l}_{L2}}^2 \frac{2}{3} \left[J_5(m_\lambda^2, \mu_\rho^2, m_{\tilde{l}_{L2}}^2, m_{\tilde{l}_{L2}}^2, m_{\tilde{l}_{L2}}^2) \right. \\
&\left. - m_\lambda \mu_\rho \tan \gamma I_5(m_\lambda^2, \mu_\rho^2, m_{\tilde{l}_{L2}}^2, m_{\tilde{l}_{L2}}^2, m_{\tilde{l}_{L2}}^2) \right] \\
&- \frac{g'^2 c_L^2 2 m_\mu^2}{8\pi^2} m_{\tilde{l}_{L2}}^2 \frac{2}{27} \left[J_5(m_B^2, \mu_\rho^2, m_{\tilde{l}_{L2}}^2, m_{\tilde{l}_{L2}}^2, m_{\tilde{l}_{L2}}^2) \right. \\
&\left. - m_B \mu_\rho \tan \gamma I_5(m_B^2, \mu_\rho^2, m_{\tilde{l}_{L2}}^2, m_{\tilde{l}_{L2}}^2, m_{\tilde{l}_{L2}}^2) \right] \\
&+ [L_2 \rightarrow L_3, R_2 \rightarrow R_3, c_L^2 \rightarrow s_L^2, c_{\nu_R}^2 \rightarrow s_{\nu_R}^2, c_{\nu_L}^2 \rightarrow s_{\nu_L}^2], \tag{30}
\end{aligned}$$

$$\begin{aligned}
a_{\mu R}^{(b)} &= -\frac{g'^2 c_R^2 m_\mu^2}{8\pi^2} m_{\tilde{l}_{R2}}^2 \frac{2}{9} \left[-J_5(m_B^2, \mu_\rho^2, m_{\tilde{l}_{R2}}^2, m_{\tilde{l}_{R2}}^2, m_{\tilde{l}_{R2}}^2) \right. \\
&\left. + m_B \mu_\rho \tan \gamma I_5(m_B^2, \mu_\rho^2, m_{\tilde{l}_{R2}}^2, m_{\tilde{l}_{R2}}^2, m_{\tilde{l}_{R2}}^2) \right] \\
&+ [R_2 \rightarrow R_3, c_R^2 \rightarrow s_R^2]. \tag{31}
\end{aligned}$$

$$\begin{aligned}
a_{\mu LR}^{(c)} &= \frac{g'^2 m_\mu^2 m_B^3}{8\pi^2} \left[\left(\frac{m_\tau}{m_\mu} \left[c_R^2 s_{LC} A_{\mu\tau}^R + s_R c_R c_L^2 A_{\mu\tau}^L + s_R c_R s_{LC} \left(A_\tau + \frac{\mu_\rho \tan \gamma}{2} \right) \right] \right. \right. \\
&+ c_R^2 c_L^2 \left[A_\mu + \frac{\mu_\rho \tan \gamma}{2} \right] \left. \right) I_5(m_B^2, m_B^2, m_B^2, m_{\tilde{l}_{L2}}^2, m_{\tilde{l}_{R2}}^2) \\
&+ \left(\frac{m_\tau}{m_\mu} \left(-c_R^2 s_{LC} A_{\mu\tau}^R + s_R c_R s_L^2 A_{\mu\tau}^L - s_R c_R s_{LC} \left[A_\tau + \frac{\mu_\rho \tan \gamma}{2} \right] \right) \right. \\
&+ c_R^2 s_L^2 \left[A_\mu + \frac{\mu_\rho \tan \gamma}{2} \right] \left. \right) I_5(m_B^2, m_B^2, m_B^2, m_{\tilde{l}_{L3}}^2, m_{\tilde{l}_{R2}}^2) \\
&+ \left(\frac{m_\tau}{m_\mu} \left(s_R^2 s_{LC} A_{\mu\tau}^R - s_R c_R c_L^2 A_{\mu\tau}^L - s_R c_R s_{LC} \left[A_\tau + \frac{\mu_\rho \tan \gamma}{2} \right] \right) \right. \\
&+ s_R^2 c_L^2 \left[A_\mu + \frac{\mu_\rho \tan \gamma}{2} \right] \left. \right) I_5(m_B^2, m_B^2, m_B^2, m_{\tilde{l}_{L2}}^2, m_{\tilde{l}_{R3}}^2)
\end{aligned}$$

$$\begin{aligned}
& + \left(\frac{m_\tau}{m_\mu} \left[-s_R^2 s_{LC} A_{\mu\tau}^R - s_R c_R s_L^2 A_{\mu\tau}^L + s_R c_R s_{LC} \left(A_\tau + \frac{\mu_\rho \tan \gamma}{2} \right) \right] \right. \\
& \left. + s_R^2 s_L^2 \left[A_\mu + \frac{\mu_\rho \tan \gamma}{2} \right] \right) I_5(m_B^2, m_B^2, m_B^2, m_{\tilde{l}_{L3}}^2, m_{\tilde{l}_{R3}}^2), \tag{32}
\end{aligned}$$

where s_L, c_L and s_R, c_R are the mixing angles that related between flavour states $\tilde{\mu}_L, \tilde{\tau}_L, \tilde{\mu}_L^c, \tilde{\tau}_L^c$ and the mass states $\tilde{l}_{L_2}, \tilde{l}_{L_3}, \tilde{l}_{R_2}, \tilde{l}_{R_3}$, namely

$$\begin{aligned}
\tilde{\mu}_L &= c_L \tilde{l}_{L_2} - s_L \tilde{l}_{L_3}, \quad \tilde{\tau}_L = s_L \tilde{l}_{L_2} + c_L \tilde{l}_{L_3}, \\
\tilde{\mu}_L^c &= c_R \tilde{l}_{R_2} - s_R \tilde{l}_{R_3}, \quad \tilde{\tau}_L^c = s_R \tilde{l}_{R_2} + c_R \tilde{l}_{R_3}.
\end{aligned}$$

with $c_L = \cos \theta_L, s_L = \sin \theta_L, c_R = \cos \theta_R, s_R = \sin \theta_R$. $A_\mu, A_{\mu\tau}^{L,R}$ are the couplings of the smuon-smuon-neutral Higgs, smuon-stauon-neutral Higgs, respectively. More details on the symbol, an interested reader can see in [27].

VII. NUMERICAL CALCULATION

The full parameter space of the SUSYE331 model contains dozens of parameters however we can classify in categories: B/μ -term: μ_ρ ; the ratio of two vacua: $\tan \gamma$; gauginos mass m_B, m_λ ; right-handed slepton mass: $m_{\tilde{l}_{R_2}}, m_{\tilde{\nu}_{R_2}}, m_{\tilde{l}_{R_3}}, m_{\tilde{\nu}_{R_3}}$; left-handed slepton mass: $m_{\tilde{l}_{L_2}}, m_{\tilde{\nu}_{L_2}}, m_{\tilde{l}_{L_3}}, m_{\tilde{\nu}_{L_3}}$; mixing terms: $A_\mu, A_\tau, A_{\tau\mu}^L, A_{\tau\mu}^R$. To simplify our calculation we can first make a rough estimation by taking the limit of $m_{\tilde{L}}, m_B, m_\lambda, \mu_\rho$ to m_{SUSY} and since A_τ , and $A_{\mu\tau}^{L,R}$ are non-diagonal terms in mixing matrix meaning A_τ , and $A_{\mu\tau}^{L,R}$ are very small then we can approximate $A_\tau = A_{\mu\tau}^{L,R} = 0$.

In this limit, the analytical expressions (28),(29),(30),(31),(32) can be written simply as follows

$$\begin{aligned}
a_{\mu L}^{(a)} &= -\frac{1}{18} \frac{g^2}{8\pi^2} \frac{m_\mu^2}{m_{SUSY}^2} + \frac{1}{54} \frac{1}{12} \frac{g'^2}{8\pi^2} \frac{m_\mu^2}{m_{SUSY}^2}, \\
a_{\mu R}^{(a)} &= \frac{1}{6} \frac{1}{12} \frac{g'^2}{8\pi^2} \frac{m_\mu^2}{m_{SUSY}^2}, \\
a_{\mu L}^{(b)} &= \frac{1}{12} \frac{g^2}{4\pi^2} \frac{m_\mu^2}{m_{SUSY}^2} + \frac{1}{4} \frac{g^2}{4\pi^2} \frac{m_\mu^2}{m_{SUSY}^2} sign(\mu_\rho) \tan \gamma - \frac{1}{12} \frac{2}{3} \frac{g^2}{8\pi^2} \frac{m_\mu^2}{m_{SUSY}^2} (1 + sign(\mu_\rho) \tan \gamma) \\
& + \frac{1}{12} \frac{4}{27} \frac{g'^2}{8\pi^2} \frac{m_\mu^2}{m_{SUSY}^2} (1 + sign(\mu_\rho) \tan \gamma), \\
a_{\mu R}^{(b)} &= -\frac{1}{12} \frac{2}{9} \frac{g'^2}{8\pi^2} \frac{m_\mu^2}{m_{SUSY}^2} (1 + sign(\mu_\rho) \tan \gamma), \\
a_{\mu LR}^{(c)} &= \frac{1}{12} \frac{1}{9} \frac{g'^2}{8\pi^2} \frac{m_\mu^2}{m_{SUSY}^3} Re \left[A_\mu + \frac{m_{SUSY} sign(\mu_\rho) \tan \gamma}{2} \right].
\end{aligned}$$

If we assume $A_\mu = 0$ then summing all above terms we have

$$\begin{aligned}\Delta a_\mu^{total} &= -\frac{1}{36} \frac{g^2}{8\pi^2} \frac{m_\mu^2}{m_{SUSY}^2} + \frac{1}{108} \frac{g'^2}{8\pi^2} \frac{m_\mu^2}{m_{SUSY}^2} + \frac{4}{9} \frac{g^2}{8\pi^2} sign(\mu_\rho) \tan \gamma \frac{m_\mu^2}{m_{SUSY}^2} \\ &+ \frac{1}{648} \frac{g'^2}{8\pi^2} sign(\mu_\rho) \tan \gamma \frac{m_\mu^2}{m_{SUSY}^2}.\end{aligned}\quad (33)$$

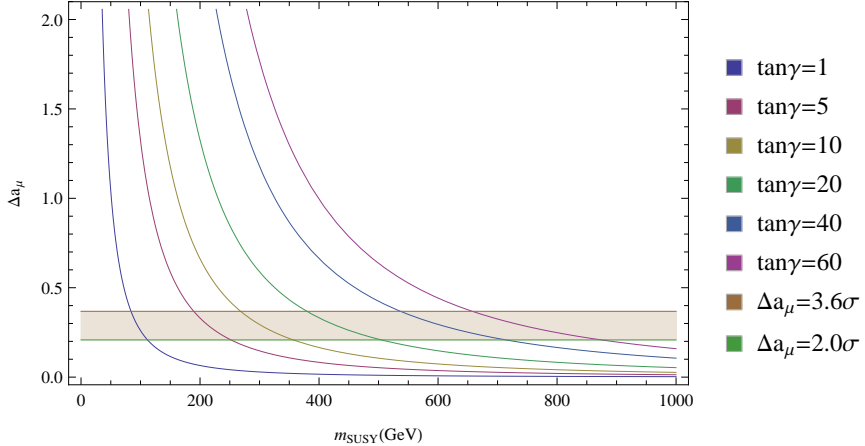


FIG. 1: Δa_μ plot against m_{SUSY}

First let us numerically estimate Δa_μ by using the Eq.(33). From Eq. (33) we can conclude that Δa_μ is the same sign with $sign(\mu_\rho)$. In Fig. 1 we plot the discrepancy of the muon MDM between experimental data and that predicted by the SM. For our convenience we have scale up the value of MDM by factor of 10^8 through out this paper. The shade region is 1.6σ difference with upper bound and lower bound are $2.0-3.6\sigma$, respectively. The muon MDM is investigated with different values of $\tan \gamma = 1, 5, 10, 20, 40, 60$. As we can see that to explain the $\geq 3.6\sigma$ difference the mass of supersymmetric particle can be as small as ≈ 75 GeV provided a value of $\tan \gamma = 1$. This is because in the SUSYE331 model, the number of new particles is increased comparing to the MSSM. Therefore the contribution to the total value of MDM is large even in the case of small $\tan \gamma$. When $\tan \gamma$ is large ($\tan \gamma=60$) the mass of the SUSY particle m_{SUSY} is limited to 900 GeV in order to address the 2.0σ discrepancy. As pointed out in [33] the simple extended of gauge symmetry model of the SM cannot address the problem of MDM because of the damped term $\frac{m_\mu^2}{M_{NP}^2}$ where M_{NP} is the mass of the new physics particle. However in the supersymmetric version of the 3-3-1 model, the contribution to the MDM of the new particle is enhanced with a factor of the ratio of two vacuum $\tan \gamma$. Therefore the issue of the MDM can be addressed with an

suitable value of $\tan \gamma$.

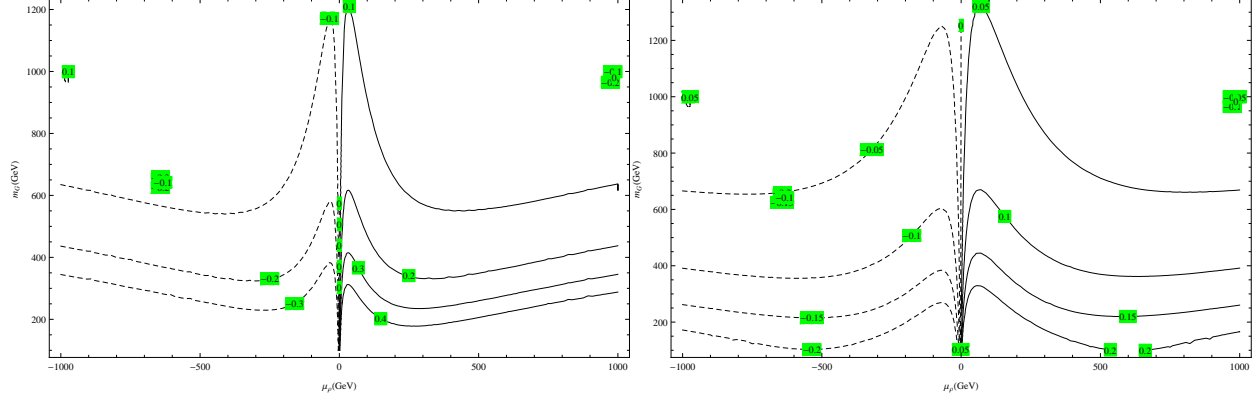


FIG. 2: Δa_μ plotted against μ_ρ and m_G

$$\begin{aligned} m_{\tilde{l}_2} &= m_{\tilde{l}_{L_2}} = m_{\tilde{l}_{R_2}} = m_{\tilde{\nu}_{L_2}} = m_{\tilde{\nu}_{R_2}}, \\ m_{\tilde{l}_3} &= m_{\tilde{l}_{L_3}} = m_{\tilde{l}_{R_3}} = m_{\tilde{\nu}_{L_3}} = m_{\tilde{\nu}_{R_3}}, \\ \tan \gamma &= 5, m_{\tilde{l}_2} = 100 \text{ GeV}, m_{\tilde{l}_3} = 1 \text{ TeV}, \\ m_B &= m_\lambda = m_G, \\ \theta_L &= \theta_R = \frac{\pi}{4}, \theta_{\nu_L} = \theta_{\nu_R} = \frac{\pi}{4}. \end{aligned}$$

FIG. 3: Δa_μ plotted against μ_ρ and m_G

$$\begin{aligned} m_{\tilde{l}_2} &= m_{\tilde{l}_{L_2}} = m_{\tilde{l}_{R_2}} = m_{\tilde{\nu}_{L_2}} = m_{\tilde{\nu}_{R_2}}, \\ m_{\tilde{l}_3} &= m_{\tilde{l}_{L_3}} = m_{\tilde{l}_{R_3}} = m_{\tilde{\nu}_{L_3}} = m_{\tilde{\nu}_{R_3}}, \\ \tan \gamma &= 5, m_{\tilde{l}_2} = 200 \text{ GeV}, m_{\tilde{l}_3} = 1 \text{ TeV}, \\ m_B &= m_\lambda = m_G, \\ \theta_L &= \theta_R = \frac{\pi}{4}, \theta_{\nu_L} = \theta_{\nu_R} = \frac{\pi}{4}. \end{aligned}$$

Next, we show the SUSYE331 contribution to the muon MDM by using the analytical expressions (28)-(32) and fixing the value of $\tan \gamma$ and slepton masses. We have assumed that $m_{\tilde{l}_2} = m_{\tilde{l}_{L_2}} = m_{\tilde{l}_{R_2}} = m_{\tilde{\nu}_{L_2}} = m_{\tilde{\nu}_{R_2}}$ and $m_{\tilde{l}_3} = m_{\tilde{l}_{L_3}} = m_{\tilde{l}_{R_3}} = m_{\tilde{\nu}_{L_3}} = m_{\tilde{\nu}_{R_3}}$. Mass hierarchy between the second and the third generation is taken in to account. Since the MSSM is embedded in the SUSYE331 then we can take the constraint on smuon mass [1] where mass of smuon is greater than 91 GeV (ABBIENDI 04). We have approximated the mass of the second generation $m_{\tilde{l}_2} = 100$ GeV and other cases $m_{\tilde{l}_2} = 200$ GeV while the mass of the third generation $m_{\tilde{l}_3}$ about 1TeV. The results obtained in Fig. 1 show that if the SUSY masses are fixed in $100 - 200$ GeV, the values of $\tan \gamma$ equals 5 in order to fit the experimental results. Hence we study the SUSY contribution to the muon MDM for fixing values of slepton masses and in the m_G and μ_ρ plane. In Figs. 2 and 3 we plot the results for $\tan \gamma = 5$, bino and gauginos masses are assumed to be equal gauginos mass, $m_B = m_\lambda = m_G$. The mixing is assumed maximal, $\theta_L = \theta_R = \frac{\pi}{4}$, $\theta_{\nu_L} = \theta_{\nu_R} = \frac{\pi}{4}$. The results given in Fig. 2 are plotted for $m_{\tilde{l}_2} = 100$ GeV, $m_{\tilde{l}_3} = 1$ TeV while the results given in the Fig. 3 are plotted for $m_{\tilde{l}_2} = 200$ GeV, $m_{\tilde{l}_3} = 1$ TeV. We plot for both negative and positive values of μ_ρ . There is a slightly asymmetry in the graph which caused by terms which do

not depend on μ_ρ . We have imposed the condition of maximum value of $|\mu_\rho| \leq 1500$ GeV to avoid fine-tuning requirement for the Higgs potential. From Fig. 2 we can see that in order to address the anomalous of the muon MDM data, the mass of the gauginos are in the range of $200 \leq m_G \leq 700$ GeV and because of the set up of the masses, $\tan \gamma = 5$ is the minimum value to satisfy experimental discrepancy $2 - 3.6\sigma$. We can also learn that the value of MDM is inverse proportional to the value of μ_ρ . In the case when the mass of the second generation is taken to be 200 GeV Fig. 3, the value of MDM merely reach 2.0σ anomaly of experimental data which set the upper bound of the second generation mass to 200 GeV given the mass of the third generation 1TeV and $\tan \gamma = 5$. The results given in Figs. 2 and 3 show that if we take a larger value of $m_{\tilde{l}_2}$, the SUSYE331 contribution to the muon MDM is enhanced in the small m_G region.

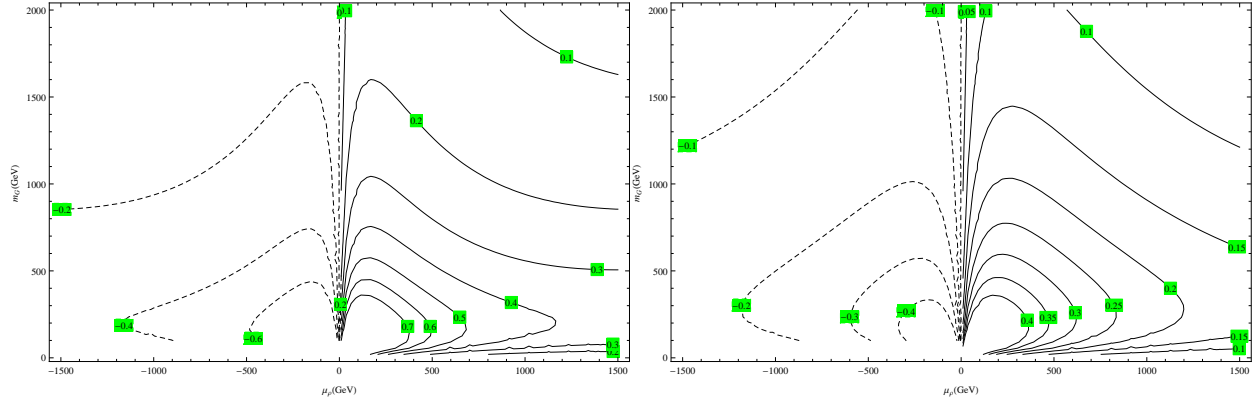


FIG. 4: Δa_μ plotted against μ_ρ and m_G

$$\begin{aligned} m_{\tilde{l}_2} &= m_{\tilde{l}_{L_2}} = m_{\tilde{l}_{R_2}} = m_{\tilde{\nu}_{L_2}} = m_{\tilde{\nu}_{R_2}}, \\ m_{\tilde{l}_3} &= m_{\tilde{l}_{L_3}} = m_{\tilde{l}_{R_3}} = m_{\tilde{\nu}_{L_3}} = m_{\tilde{\nu}_{R_3}}, \\ \tan \gamma &= 60, m_{\tilde{l}_2} = 500 \text{ GeV}, m_{\tilde{l}_3} = 2 \text{ TeV}, \\ m_B &= m_\lambda = m_G, \\ \theta_L &= \theta_R = \frac{\pi}{4}, \theta_{\nu_L} = \theta_{\nu_R} = \frac{\pi}{4}. \end{aligned}$$

FIG. 5: Δa_μ plotted against μ_ρ and m_G

$$\begin{aligned} m_{\tilde{l}_2} &= m_{\tilde{l}_{L_2}} = m_{\tilde{l}_{R_2}} = m_{\tilde{\nu}_{L_2}} = m_{\tilde{\nu}_{R_2}}, \\ m_{\tilde{l}_3} &= m_{\tilde{l}_{L_3}} = m_{\tilde{l}_{R_3}} = m_{\tilde{\nu}_{L_3}} = m_{\tilde{\nu}_{R_3}}, \\ \tan \gamma &= 60, m_{\tilde{l}_2} = 800 \text{ GeV}, m_{\tilde{l}_3} = 2 \text{ TeV}, \\ m_B &= m_\lambda = m_G, \\ \theta_L &= \theta_R = \frac{\pi}{4}, \theta_{\nu_L} = \theta_{\nu_R} = \frac{\pi}{4}. \end{aligned}$$

Remember that the SUSYE331 contribution to the muon MDM is proportional to $\tan \gamma$. The results given in Fig.1 show that if the $\tan \gamma = 60$, the interested m_{SUSY} region is $[600, 800]$ GeV. We impose the upper bound for $\tan \gamma = 60$ (ACHARD 04) [1]. Hence, we numerically study the SUSYE331 contribution to the muon MDM in the case $\tan \gamma = 60$ and the slepton mass hierarchy between the second and third family is retained. In Fig.4, and Fig.5 we plot muon MDM on the m_G and μ_ρ plane with the same condition as above

except the mass of the generation is taken to be 500 GeV for Fig. 4 and 800 GeV for Fig. 5 respectively and the mass of the third generation to be 2TeV. The result given in the Fig.4 show that the upper bound for $m_G = 1500$ GeV and $\mu_\rho = 1500$ GeV. However the results given in the Fig.5 set the upper bound for $m_G = 1100$ GeV and $\mu_\rho = 1200$ GeV, respectively.

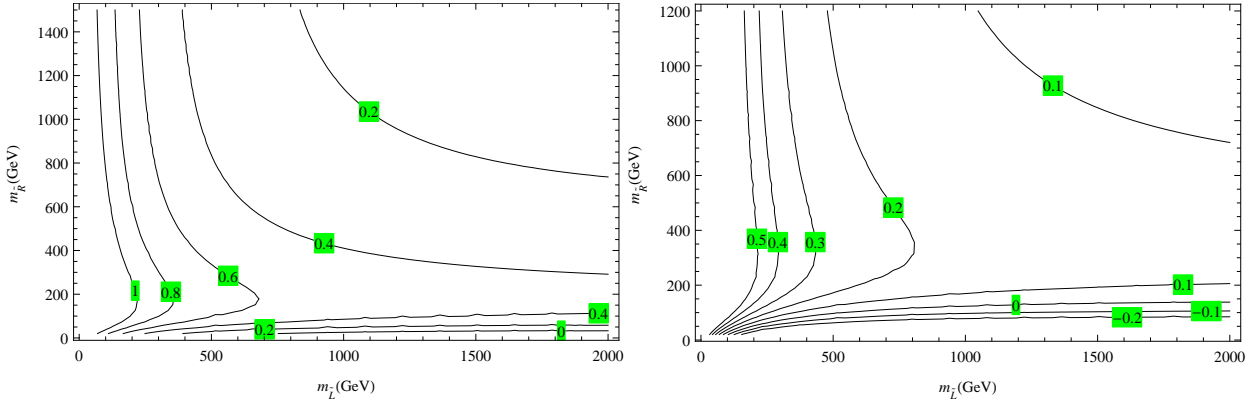


FIG. 6: Δa_μ plot against $m_{\tilde{L}}$ and $m_{\tilde{R}}$.

$$\begin{aligned} m_{\tilde{l}_{L_2}} &= m_{\tilde{\nu}_{L_2}} = m_{\tilde{l}_{L_3}} = m_{\tilde{\nu}_{L_3}} = m_{\tilde{L}}, \\ m_{\tilde{l}_{R_2}} &= m_{\tilde{\nu}_{R_2}} = m_{\tilde{l}_{R_3}} = m_{\tilde{\nu}_{R_3}} = m_{\tilde{R}}, \\ \tan \gamma &= 60, \mu_\rho = 140 \text{ GeV}, m_\lambda = 1 \text{ TeV} \end{aligned}$$

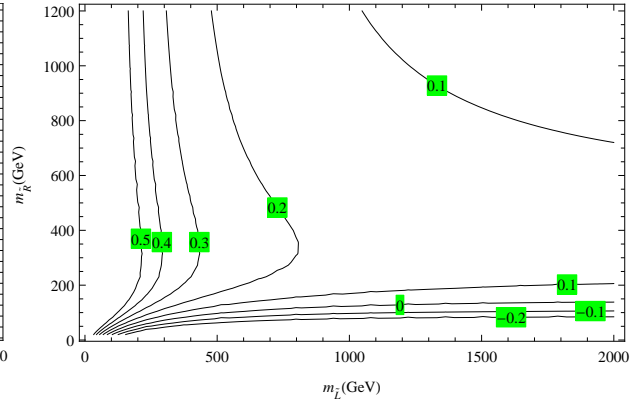


FIG. 7: Δa_μ plot against $m_{\tilde{L}}$ and $m_{\tilde{R}}$.

$$\begin{aligned} m_{\tilde{l}_{L_2}} &= m_{\tilde{\nu}_{L_2}} = m_{\tilde{l}_{L_3}} = m_{\tilde{\nu}_{L_3}} = m_{\tilde{L}}, \\ m_{\tilde{l}_{R_2}} &= m_{\tilde{\nu}_{R_2}} = m_{\tilde{l}_{R_3}} = m_{\tilde{\nu}_{R_3}} = m_{\tilde{R}}, \\ \tan \gamma &= 60, \mu_\rho = 140 \text{ GeV}, m_\lambda = 2 \text{ TeV} \end{aligned}$$

Next we will take into account the current upper bound of the mass of Bino 350 GeV at the mass of top quark 174 GeV based on CP violating phase [1]. We have set $m_{\tilde{l}_{L_2}} = m_{\tilde{\nu}_{L_2}} = m_{\tilde{l}_{L_3}} = m_{\tilde{\nu}_{L_3}} = m_{\tilde{L}}$ and $m_{\tilde{l}_{R_2}} = m_{\tilde{\nu}_{R_2}} = m_{\tilde{l}_{R_3}} = m_{\tilde{\nu}_{R_3}} = m_{\tilde{R}}$ and $\tan \gamma = 60, \mu_\rho = 140$ GeV. The mass of other gauginos m_λ is set to be 1 TeV (Fig.6) and 2 TeV (Fig.7). These figures illustrate the effects of varying $m_{\tilde{L}}, m_{\tilde{R}}$ to the SUSYE331 contribution to the muon MDM. Combining the muon MDM from experimental and the theoretical predicted given in the (6) and (7), we obtain the interested region of the parameter space. Especially, the region of the parameter space of $m_{\tilde{R}}$ is very large $m_{\tilde{R}} > 20$ GeV while that of $m_{\tilde{L}}$ is slightly constrained and depends on the value of gaugino mass. If we fixed $m_\lambda = 1$ TeV the results given in Fig.6 show the lower bound of $m_{\tilde{L}} \simeq 400$ GeV and there is no upper bound for $m_{\tilde{R}}$. From Fig. 7 we can find the upper bound mass of the left slepton $m_{\tilde{L}} \leq 800$ GeV.

Furthermore, by choosing the upper bound for the left-handed slepton mass above of third generation $m_{\tilde{l}_{L_3}} = m_{\tilde{l}_{R_3}} = m_{\tilde{\nu}_{L_3}} = m_{\tilde{\nu}_{R_3}} = 800$ GeV and fixing $\tan \gamma = 60, \mu_\rho = 140$ GeV, $m_B = 350$ GeV, we plot the SUSYE331 contribution to the muon MDM on the plane of $m_{\tilde{l}_{L_2}} = m_{\tilde{\nu}_{L_2}} = m_{L_2}$, $m_{\tilde{l}_{R_2}} = m_{\tilde{\nu}_{R_2}} = m_{R_2}$ in Fig.8 and Fig.9. The results for the cases of

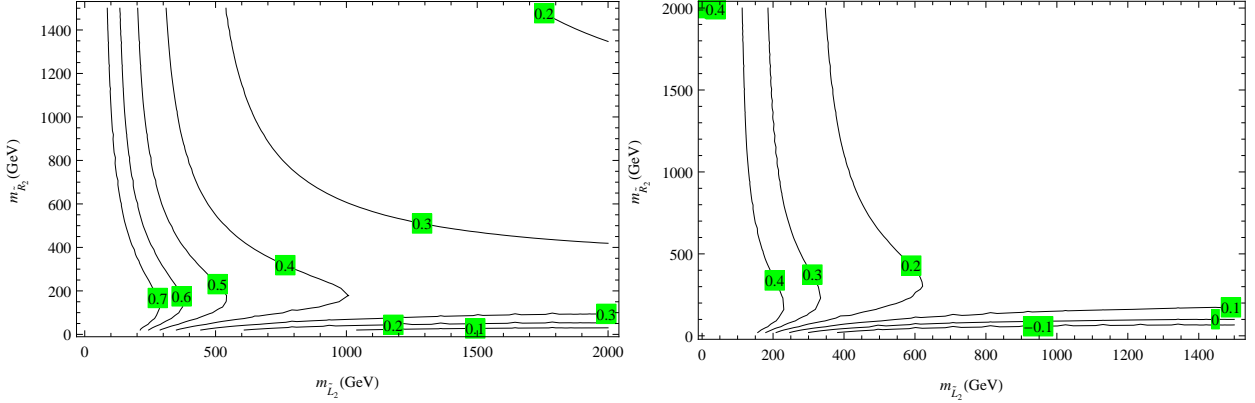


FIG. 8: Δa_μ plot against $m_{\tilde{L}_2}$ and $m_{\tilde{R}_2}$.

$$m_{\tilde{l}_{L2}} = m_{\tilde{\nu}_{L2}} = m_{L2}, \quad m_{\tilde{l}_{R2}} = m_{\tilde{\nu}_{R2}} = m_{R2}$$

$$m_{\tilde{l}_{L3}} = m_{\tilde{l}_{R3}} = m_{\tilde{\nu}_{L3}} = m_{\tilde{\nu}_{R3}} = 800 \text{ GeV}$$

$$\tan \gamma = 60, \mu_\rho = 140 \text{ GeV}, m_B = 350 \text{ GeV}$$

FIG. 9: Δa_μ plot against $m_{\tilde{L}_2}$ and $m_{\tilde{R}_2}$.

$$m_{\tilde{l}_{L2}} = m_{\tilde{\nu}_{L2}} = m_{L2}, \quad m_{\tilde{l}_{R2}} = m_{\tilde{\nu}_{R2}} = m_{R2}$$

$$m_{\tilde{l}_{L3}} = m_{\tilde{l}_{R3}} = m_{\tilde{\nu}_{L3}} = m_{\tilde{\nu}_{R3}} = 800 \text{ GeV}$$

$$\tan \gamma = 60, \mu_\rho = 140 \text{ GeV}, m_B = 350 \text{ GeV}$$

$m_\lambda = 1 \text{ TeV}$ and $m_\lambda = 2 \text{ TeV}$ are shown in Fig.8 and Fig.9, respectively. Comparing with the experimental results, we find the lower bound of the $m_{L2} > 500 \text{ GeV}$ for fixing $m_\lambda = 1 \text{ TeV}$ and the upper bound for the mass of the left-handed slepton of the second generation is 600 GeV for fixing $m_\lambda = 2 \text{ TeV}$. There is no bound of the right-handed slepton mass of the second generation.

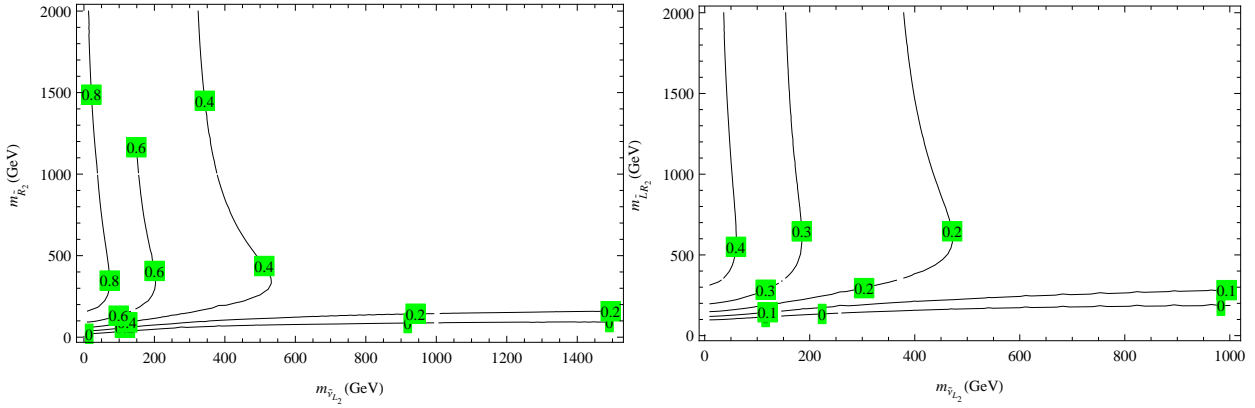


FIG. 10: Δa_μ plot against $m_{\tilde{\nu}_{L2}}$ and $m_{\tilde{R}_2}$.

$$\theta_R = \theta_L = 0 \text{ and } \theta_{\nu_R} = \theta_{\nu_L} = \frac{\pi}{4},$$

$$\tan \gamma = 60, \mu_\rho = 140 \text{ GeV},$$

$$m_{R3} = 800 \text{ GeV}, \quad m_{\tilde{L}_2} = 600 \text{ GeV},$$

$$m_B = 350 \text{ GeV}, \quad m_\lambda = 1 \text{ TeV}$$

FIG. 11: Δa_μ plot against $m_{\tilde{\nu}_{L2}}$ and $m_{\tilde{R}_2}$.

$$\theta_R = \theta_L = 0 \text{ and } \theta_{\nu_R} = \theta_{\nu_L} = \frac{\pi}{4},$$

$$\tan \gamma = 60, \mu_\rho = 140 \text{ GeV},$$

$$m_{R3} = 800 \text{ GeV}, \quad m_{\tilde{L}_2} = 600 \text{ GeV},$$

$$m_B = 350 \text{ GeV}, \quad m_\lambda = 2 \text{ TeV}$$

We have investigated the maximal mixing case in which $\theta_{\nu_R} = \theta_{\nu_L} = \frac{\pi}{4}$ are related to neutrino mixing and $\theta_R = \theta_L = \frac{\pi}{4}$ are related to charge lepton mixing. Next, we will investigate smaller case $\theta_R = \theta_L = 0$ and $\theta_{\nu_R} = \theta_{\nu_L} = \frac{\pi}{4}$. In Figs. 10 and 11 we have plotted the MDM on the $m_{\tilde{\nu}_{L_2}}$ and m_{R_2} where we have used the above constraint for $m_{\tilde{L}_2} = 600$ GeV and other parameters are fixed as: $\tan \gamma = 60$, $\mu_\rho = 140$ GeV, $m_{R_3} = 800$ GeV, $m_B = 350$ GeV, $m_\lambda = 1$ TeV for the left -side figure and $m_\lambda = 2$ TeV for the right-side figure. The mass of the sneutrino has to be smaller than 550 GeV to address $2 - 3.6 \sigma$ discrepancy if $m_\lambda = 2$ TeV. The lower bound of the right-handed slepton mass of the second generation is around tens of GeV for fixing $m_\lambda = 1$ TeV and is a hundred GeV for fixing $m_\lambda = 2$ TeV.

VIII. CONCLUSIONS

In this paper we have examined in detail the muon $g - 2$ in the frame work of the SUSYE331 model. We calculated one-loop SUSYE331 contributions to the muon MDM based on both the mass eigenstate and the weak eigenstate methods. The mass eigenstates of the neutralino and chargino are obtained using approximation method. To recognize the effects of the SUSYE331 parameters to the muon MDM , we work with the analytical expressions of the muon MDM based on the mass insertion method. We have considered all parameters of SUSYE331 as free parameters. In our calculation we have made some assumptions: maximal mixing, mixing terms A_τ, A_μ , and $A_{\mu\tau}^{L,R}$ are small and are neglected in our calculation. In particularly, by taking the limit $\mu_\rho, m_\lambda, m_{\tilde{L}}, m_B$ to m_{SUSY} we obtain the reduced analytical expressions of the contribution of the SUSYE331 to the muon MDM. Results show that the SUSYE331 contribution to the muon MDM is enhanced in the small region of the m_{SUSY} and the large values of the $\tan \gamma$. We have investigated for both small and large values of ratio of two vacua $\tan \gamma$. The numerical results show that in order to consist with the experimental bound of the muon MDM , the $m_{SUSY} \simeq 75$ GeV for $\tan \gamma = 1$ and $m_{SUSY} = 900$ for $\tan \gamma = 60$. On the other hand, we also investigated the SUSYE33 contribution to the muon MDM in the case of the mass hierarchy between the second and the third generation. In the case which $\tan \gamma$ is small ($\tan \gamma = 5$) and one generation of the slepton mass is fixed at the $\mathcal{O}(1)$ TeV, the light slepton particle mass is bounded from 100 GeV to 200 GeV and Δa^μ can be comparable with the current limit on the muon MDM. When $\tan \gamma$ is large ($\tan \gamma = 60$) the mass of the light left-handed slepton particle is bound

to 800 GeV. Finally, we would like to comment on the case with the maximal flavor mixing only in the sneutrino sector, we obtain the upper bound of the mass of sneutrino is is 550 GeV. These values can be examined at LHC or furure collider ILC.

IX. FEYNMAN DIAGRAMS

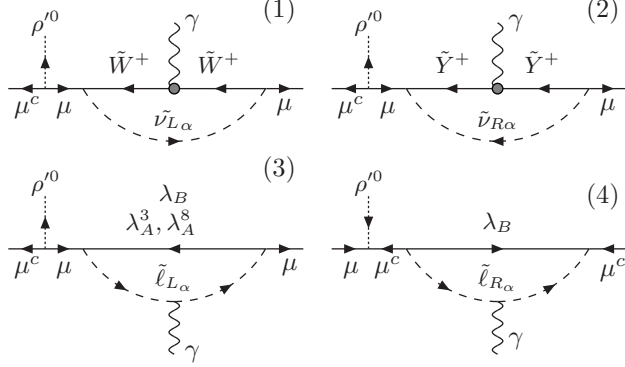


FIG. 12: Contribution to $a_{\mu L}^{(a)}$ [1 – 3] and $a_{\mu R}^{(a)}$ [4]

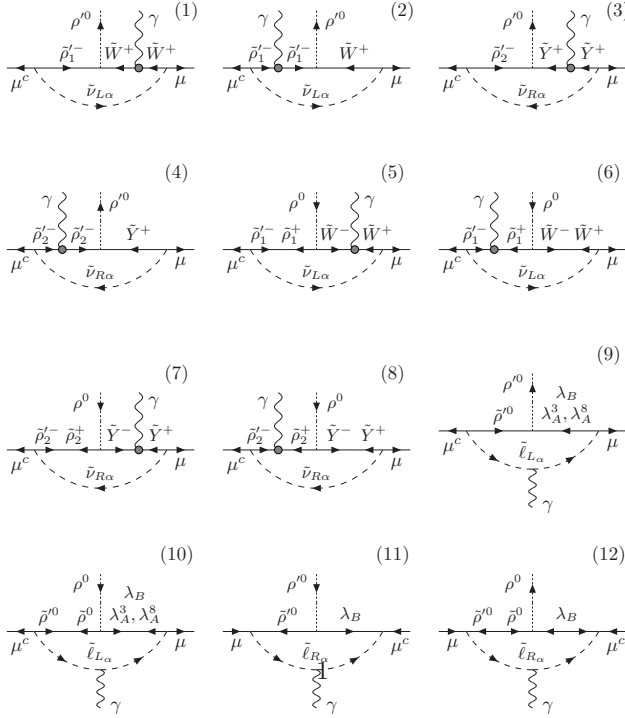


FIG. 13: Contribution to $a_{\mu L}^{(b)}$ [1 – 10] and $a_{\mu R}^{\mu(b)}$ [11 – 12]

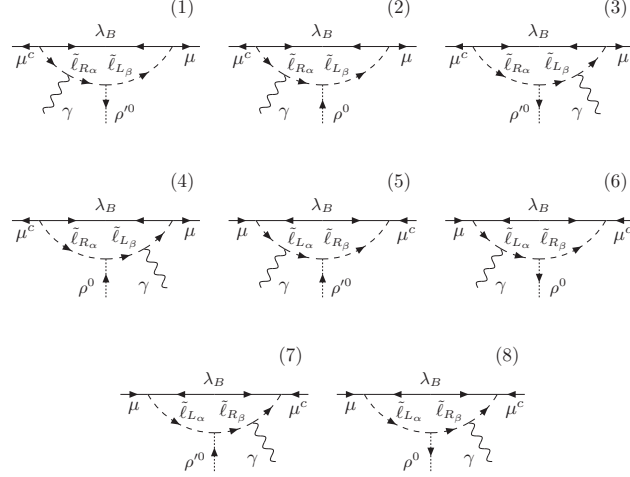


FIG. 14: Contribution to $a_{\mu L}^{(c)}[1 - 6]$ and $a_{\mu R}^{(c)}[7 - 8]$

Acknowledgments

D. T. Binh thanks Le Tho Hue for his suggestion. This research is funded by Vietnam National Foundation for Science and Technology Development (NAFOSTED) under grant number 103.01-2014.51.

¹

X. APPENDIX SECTION

In this section we will define some integrals used in our calculation. The following integral is defined in [34].

$$\begin{aligned} I^{(N)}(\nu_i; \nu_j) &\equiv \int \frac{d^D k}{(k^2 - m_1^2)^{\nu_1} \dots (k^2 - m_N^2)^{\nu_N}} \\ &= \int \frac{d^D k}{\prod_{j=1}^N (k^2 - m_j^2)^{\nu_j}} \end{aligned}$$

In special case $D = 4$ and there are two masses, we have:

$$\begin{aligned} I^{(2)}(\nu_1, \nu_2; m_1, m_2) &= \pi^2 i^{-3} (-m_2)^{2-\nu_1-\nu_2} \frac{\Gamma(\nu_1 + \nu_2 - 2)}{\Gamma(\nu_1 + \nu_2)} \\ &\times {}_2F_1(\nu_1 + \nu_2 - 2, \nu_1; \nu_1 + \nu_2; 1 - \frac{m_1^2}{m_2^2}) \end{aligned}$$

The loop integrals are defined as :

$$I_N(m_1^2, \dots, m_N^2) = \frac{i}{\pi^2} \int \frac{d^4 k}{(k_1^2 - m_1^2) \dots (k_N^2 - m_N^2)},$$

$$J_N(m_1^2, \dots, m_N^2) = \frac{i}{\pi^2} \int \frac{k^2 d^4 k}{(k_1^2 - m_1^2) \dots (k_N^2 - m_N^2)}.$$

- [1] J. Beringer et al, (Particle Data Group), Phys. Rev. D **86**, 010001 (2012).
- [2] H. N. Long, Phys. Rev. D **54** (1996) 4691.
- [3] F. Pisano, V. Pleitez, Phys. Rev. D 46 (1992) 410,
- [4] R. Foot, H. N. Long, T. A. Tran, Phys. Rev. D **50** (1994) R34.
- [5] C. A. de S. Pires, P. S. Rodrigues da Silva, JCAP 0712 (2007) **012**.
- [6] J. K. Mizukoshi, C. A. de S. Pires, F. S. Queiroz, P. S. R. da Silva, Phys. Rev. D 83 (2011) 065024.
- [7] F. Queiroz, C. A. de S. Pires, P. S. R. da Silva, Phys. Rev. D **82** (2010) 065018.
- [8] D. Cogollo, A. V. de Andrade, F. S. Queiroz and P. Rebello Teles, Eur. Phys. J. C **72**, 2029 (2012).
- [9] J. D. Ruiz-Alvarez, C. A. de S. Pires, F. S. Queiroz, D. Restrepo and P. S. Rodrigues da Silva, Phys. Rev. D **86**, 075011 (2012).
- [10] P. V. Dong, H. N. Long and H. T. Hung, Phys. Rev. D **86**, 033002 (2012)
- [11] A. Alves, E. Ramirez Barreto, A. G. Dias, C. A. de S. Pires, F. S. Queiroz and P. S. Rodrigues da Silva, Eur. Phys. J. C **73**, 2288 (2013).
- [12] P. V. Dong, H. T. Hung, T. D. Tham , Phys. Rev. D **87** (2013) 115003.
- [13] P. V. Dong, T. Phong Nguyen, D. V. Soa, Phys. Rev. D **88**, 095014 (2013).
- [14] P. V. Dong, H. N. Long, D. T. Nhungh and D. V. Soa, Phys. Rev. D 73, 035004 (2006).
- [15] D. T. Huong, P. V. Dong, C. S. Kim, N. T. Thuy, Phys. Rev. D, 91, 055023 (2015); P. V Dong, D. T. Huong, Farinaldo S. Queiroz, N. T. Thuy, Phys. Rev. D 90, 075021 (2014)
- [16] C.A. de S. Pires, P. S. Rodrigues da Silva, Phys. Rev. D 64 (2001) 117701.
- [17] C.A. De Sousa Pires, P. S. Rodrigues da Silva, Phys. Rev. D 65 (2002) 076011.
- [18] N. A. Ky, H. N. Long, D. V. Soa, Phys. Lett. B 486 (2000) 140.
- [19] C. Kelso, P. R. D. Pinheiro, F. S. Queiroz, W. Shepherd. Eur. Phys. J. C 74 (2014) 2808.
- [20] Chris Kelso, H. N. Long, R. Martinez, Farinaldo S. Queiroz, *Phys. Rev. D* **90**, 113011 (2014).
- [21] M.J.G. Veltman, Acta Phys. Pol. B12(1981)437.
- [22] P. Langacker, M. Luo, Phys. Rev. D44 (1991) 817.

- [23] P. Fayet, in Unification of the Fundamental Particles Interactions, edited by S. Ferrara, J. Ellis and P. van Nierwenhuizen (Plenum, New York, 1980) p. 587; J.A. Grifols and A. Mendez, Phys. Rev. D26 (1982) 1809; J. Ellis, J. S. Hagelin and D. V. Nanopoulos, Phys. Lett. B166 (1982) 283; R. Barbieri and L. Maiani, Phys. Lett. B117 (1982) 203; D. A. Kosower, L. M. Krauss and N. Sakai, Phys. Lett. B133 (1983) 305; T. C. Yuan, R. Arnowitt, A. H. Chamseddine and P. Nath, Z. Phys. C26 (1984) 407; J. C. Romao, A. Barroso, M. C. Bento and G. C. Branco, Nucl. Phys. B 250 (1985) 295; J. Lopez, D.V. Nanopoulos and X. Wang, Phys. Rev. D 49 (1991) 366; U. Chattopadhyay and P. Nath; T. Moroi, Phys. Rev. D **53**, 6565 (1996).
- [24] J. Ellis and D. V. Nanopoulos, Phys. Lett. 110B (1982) 44; I-H. Lee, Phys. Lett. **B 138** (1984) 121; Nucl. Phys. **B 246** (1984) 120.
- [25] A. Brignole, A. Rossi, Nucl. Phys. B 701 (2004), 3-53; K. S. Babu and C. Kolda, Phys. Rev. Lett. 89 (2002) 241802; A. Abada, D. Das and C. Weiland, JHEP 1203 (2012) 100; A. Abada., D. Das, A. Vicent and C. Weiland, JHEP 1209 (2012) 015.
- [26] P. V. Dong, D. T. Huong, M. C. Rodriguez, H. N. Long, Nucl. Phys. **B 772**, 150 (2007).
- [27] P. T. Giang, L. T. Hue, D. T. Huong, H. N. Long, Nucl. Phys. **B 864** (2012) 85.
- [28] L. T. Hue, D. T. Huong, H. N. Long, Nucl. Phys. **B 873** (2013) 207.
- [29] P. V. Dong, Tr. T. Huong, N. T. Thuy, H. N. Long, *JHEP* **073**, (2007) 0711.
- [30] D. T. Huong, H. N. Long, *JHEP*, **049**, (2008) 0807.
- [31] M. Davier. et al., Eur. Phys. J. C 66 (2010) 127; A. Hoecker, B. Malaescu, C. Z. Yuan and Z. Zhang, Eur. Phys. C 66 (2010) 1.
- [32] Muon G-2 Collaboration, Phys. Rev. D 73 (2006).
- [33] A. Czarnecki and W. J. Marciano, Phys. Rev. D 64 (2001) 013014.
- [34] A. I. Davydychev, J. Math. Phys. **32** (1991) 4299.

$\Delta a_\mu \times 10^8$ plotted vs $\tan\gamma$ and M_{SUSY}

